Applied Radiation and Isotopes 67 (2009) 1897–1903

Contents lists available at ScienceDirect

Applied Radiation and Isotopes

journal homepage: www.elsevier.com/locate/apradiso

An improved method for the non-destructive characterization of radioactive waste by gamma scanning

Y.F. Bai [a,b], E. Mauerhofer [a,*], D.Z. Wang [b], R. Odoj [a]

[a] Institute of Energy Research, IEF-6: Safety Research and Reactor Technology, Forschungszentrum Jülich GmbH, 52425 Jülich, Germany
[b] School of Nuclear Science and Engineering, Shanghai Jiao Tong University, 200240 Shanghai, China

ARTICLE INFO

Article history:
Received 13 June 2008
Received in revised form
30 March 2009
Accepted 25 May 2009

Keywords:
Radioactive waste
Segmented gamma scanning
Isotope activity
Angular dependent count rate distribution

ABSTRACT

A method to improve the reliability and accuracy of activity results in segmented gamma scanning of radioactive waste drums with non-uniform isotope and matrix distribution has been developed. The improved method which is based on numerical simulations of the measured angular dependent count rate distribution during drum rotation in segmented gamma scanning has been validated through the measurement of Cs-137 and Co-60 activities in 13 real radioactive waste drums with heterogeneous activity and matrix distributions. The results were compared to that obtained for the conventional method assuming homogeneous activity and matrix distributions.

1. Introduction

Radioactive waste has to meet the specifications and acceptance criteria defined by national regulatory and management authorities for its intermediate and final storage. The non-destructive determination of the isotope specific activity content in quality checking of radioactive waste drums is most widely performed by segmented gamma scanning (SGS). Generally it is assumed that the matrix and the activity are uniformly distributed in each drum segment that is measured. Corrections for gamma attenuation in the waste matrix are usually performed by methods like density estimation by drum weighing or calculation of corrective factors based on assumptions regarding the average distribution of density and activity in the waste. However, waste drums are often heterogeneous, and span a wide range of matrix composition and activity distribution. Hence, uncertainties will be introduced which cannot be accounted for by standard correction procedures. Thus SGS errors are mainly related to non-uniform measurement responses associated with unknown radioactive sources spatial distribution and matrix heterogeneity including internal shielding structures of unknown design (Filß, 1995; Quoc Dung, 1997, 1998; Report WG-A-03, 2002).

In this paper we describe an improved method to quantify the activity of spatially concentrated gamma-emitting isotopes ('hot spots') in heterogeneous waste drums. This method is based on the analysis of the angular dependent count rate distributions recorded during the waste drum rotation in SGS to localize 'hot spots' inside the waste package and to determine the gamma attenuation properties of the waste matrix. To achieve this, numerical simulations and χ^2 fits of the angular dependent count rate distributions were performed using an analytical expression derived from a geometrical model. The application of the improved method to the quantification of non-uniform distributed Cs-137 and Co-60 activities in real heterogeneous radioactive waste drums is demonstrated.

2. The improved method

A heterogeneous waste matrix may be considered as a composite of active waste components containing 'hot spots' assimilated as point sources, and passive waste components containing shielding structures. Based on this consideration the angular dependent count rate of a collimated γ-ray detector exposed to point sources of 1 Bq activity located at different radial and angular positions (p_i,β_i) in the central horizontal section of a drum segment may be calculated in function of the rotation angle θ of the waste drum as

$$Z_\gamma(\theta) = \varepsilon_0 \cdot I_\gamma \cdot e^{-(\mu/\rho_w \cdot \rho_w \cdot d_w)} \cdot \sum_{(p_i,\beta_i)} \left(\frac{d_0}{d_i(\theta)}\right)^2 e^{-(\mu/\rho_a \cdot \rho_a \cdot l_a(\theta))} \times e^{-(\mu/\rho_s \cdot \rho_s \cdot l_s(\theta))} \cdot e^{-(\mu/\rho_c \cdot \rho_c \cdot l_c(\theta))} \quad (1)$$

where d_0 and $d_i(\theta)$ are the distances of the segment centre and of the point source from the centre of the γ-ray detector surface, respectively; ε_0 is the photopeak efficiency of the considered γ-ray

* Corresponding author. Tel.: +49 2461 61 4094; fax: +49 2461 61 2992.
E-mail address: e.mauerhofer@fz-juelich.de (E. Mauerhofer).

0969-8043/$ - see front matter © 2009 Elsevier Ltd. All rights reserved.
doi:10.1016/j.apradiso.2009.05.017

energy for a point source at the distance d_0; I_γ is the intensity of the considered γ-ray energy, ρ_w, ρ_a, ρ_s and ρ_c are the densities of the drum wall, the active waste matrix, the passive waste matrix and the collimator of the γ-ray detector, respectively, μ/ρ_w, μ/ρ_a, μ/ρ_s, μ/ρ_c are the corresponding mass attenuation coefficients at the considered γ-ray energy; d_w is the wall thickness of drum and $l_a(\theta)$, $l_s(\theta)$ and $l_c(\theta)$ are the mean distances covered by the γ-ray in the active waste matrix, the passive waste matrix and the collimator of the γ-ray detector, respectively, to reach the centre of the γ-ray detector surface. The geometric model used to evaluate $Z_\gamma(\theta)$ is shown in Fig. 1. The distance of the point source from the centre of the γ-ray detector surface is expressed by

$$d_i(\theta) = \sqrt{(d_0 - p_i\ \cos(\theta+\beta_i))^2 + (p_i\ \sin(\theta+\beta_i))^2} \tag{2}$$

where p_i and β_i are the radial and angular positions of the point source, respectively. The mean distance covered by the γ-ray in the active waste matrix is given by

$$l_a(\theta) = d_i(\theta) - \alpha\cdot d_0 + \sqrt{(\alpha\cdot d_0)^2 + (R-d_s)^2 - d_0^2} - d_w \tag{3}$$

where R is the drum radius, d_s the mean thickness of the passive matrix and α a parameter calculated as follows:

$$\alpha = \frac{d_0 - p_i\ \cos(\theta+\beta_i)}{d_i(\theta)} \tag{4}$$

The mean distance covered by the γ-ray in the passive matrix is given by

$$l_s(\theta) = d_i(\theta) - \alpha\cdot d_0 + \sqrt{(\alpha\cdot d_0)^2 + R^2 - d_0^2} - l_a(\theta) - d_w \tag{5}$$

The mean distance covered by the γ-ray in the collimator (cylindrical) of the γ-ray detector is given by

$$l_c(\theta) = 0 \quad \text{for } d_i(\theta) \le d_{col}$$
$$l_c(\theta) = \frac{L_{col}}{\alpha} - \frac{R_{col}}{\sqrt{1-\alpha^2}} \quad \text{for } d_i(\theta) > d_{col} \tag{6}$$

where L_{col} is the collimator length, R_{col} the collimator radius and d_{col} calculated as

$$d_{col} = \alpha\cdot d_i(\theta)\sqrt{1+\left(\frac{R_{col}}{L_{col}}\right)^2} \tag{7}$$

The density of the active waste matrix ρ_a in a drum segment may be expressed as

$$\rho_a = \rho_s + \frac{V}{V_a}(\rho_m - \rho_s) \tag{8}$$

where ρ_m is the apparent drum waste density determined by weighing; ρ_s is the density of the passive matrix and V and V_a are the volumes of the drum segment and of the active matrix seen by the collimated γ-ray detector, respectively. V is expressed for a cylindrical collimator by

$$V = \frac{2\cdot\pi}{3}\left(\frac{R_{col}}{L_{col}}\right)^2 (R-d_w)(3\cdot d_0^2 + (R-d_w)^2) \tag{9}$$

and V_a by

$$V_a = \frac{2\cdot\pi}{3}\left(\frac{R_{col}}{L_{col}}\right)^2 (R-d_s-d_w)(3\cdot d_0^2 + R^2 + (d_s+d_w)^2 - 2\cdot R(d_s+d_w)) \tag{10}$$

The volume of the passive matrix V_s is calculated as the difference between V and V_a.

The above equations enable to simulate the angular dependent count rate distributions for various point source configurations and different properties of the active and passive matrix and a given counting geometry. For the localization of the 'hot spots' within a drum segment and the determination of the gamma attenuation properties of the drum segment, the simulated count rates $Z_\gamma(\theta)$ are fitted to the measured count rates $T_\gamma(\theta)$ using the following χ^2 minimization:

$$\chi^2 = \sum_\theta^n \left(\frac{Z_\gamma(\theta)}{Z_\gamma(\theta)_{\max}} - \frac{T_\gamma(\theta)}{T_\gamma(\theta)_{\max}}\right)^2 \tag{11}$$

where $Z_\gamma(\theta)_{\max}$ and $T_\gamma(\theta)_{\max}$ are the maxima of the simulated and measured angular dependent count rate distributions, respectively, and n is the number of distributions recorded for a segment ($n = 360/\Delta\theta$). The lowest χ^2-value obtained from the fit of the angular dependent count rate distributions recorded for 'hot spots' at various gamma energies i.e. for different gamma-emitting isotopes will lead first to the gamma attenuation properties of the drum segment under investigation. Then a second fit of the angular dependent count rate distributions is performed to determine the radial and angular positions of the

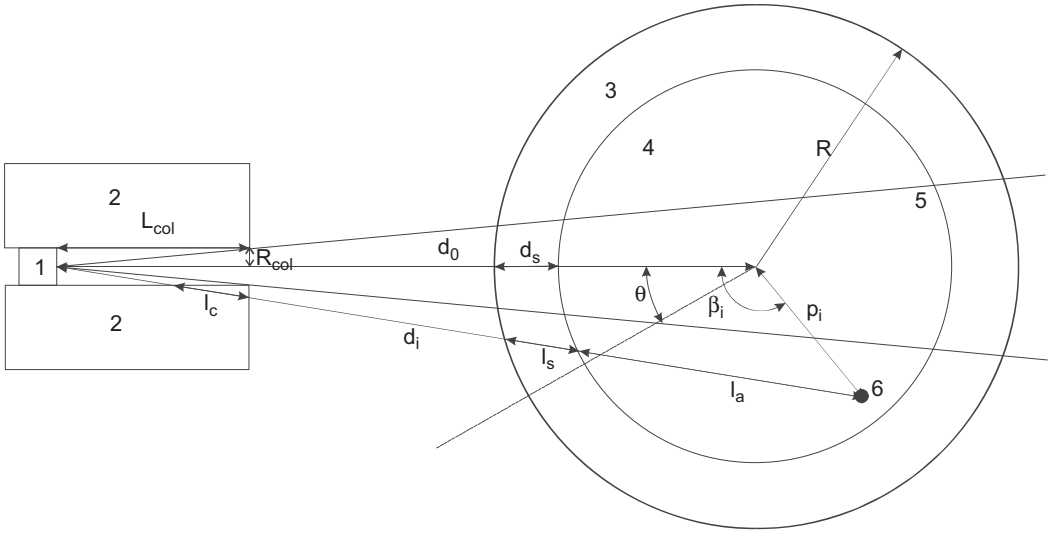

Fig. 1. Geometric model used to simulate the angular dependent count rate distributions. 1: HPGe-detector, 2: lead collimator; 3: passive matrix; 4: active matrix; 5: volume of the drum segment seen by the collimated HPGe-detector; 6: hot spot.

'hot spots' by keeping constant the gamma attenuation properties previously determined for the drum segment. Finally the 'hot spots' activity in Bq for the investigated drum segment is calculated as

$$A = \frac{\sum_{\theta}^{n} T_{\gamma}(\theta)}{\sum_{\theta}^{n} Z_{\gamma}(\theta)^{p_i,\beta_i,\rho_a,d_s}_{\chi^2_{min}}} \tag{12}$$

The relative uncertainty of the activity is estimated as

$$\sigma_A = \frac{\sqrt{n \cdot \chi^2_{min}}}{\sum_{\theta}^{n} T_{\gamma}(\theta)} \times 100 \tag{13}$$

If the angular dependent count rate distribution is homogeneous and if the gamma attenuation properties of the drum segment have been previously determined (at least one 'hot spot' analysis for an other angular dependent count rate distribution to determine the matrix properties), then the activity of the corresponding isotope in the drum segment is calculated as (Filß, 1995)

$$A = \frac{T_{\gamma}(\theta)_{mean}}{I_{\gamma} \cdot \varepsilon_0 \cdot F_0 \cdot 1 - e^{((-\mu/\rho_a)\rho_a(R-d_s-d_w)}} \times e^{((\mu/\rho_s)\rho_s \cdot d_s)} \cdot e^{((\mu/\rho_w)\rho_w \cdot d_w)} \tag{14}$$

where $T_{\gamma}(\theta)_{mean}$ is the mean value of the measured angular dependent count rate distribution and F_0 is the area of the spherical zone formed by the intersection of the (conical) volume of the drum segment seen by the collimated γ-ray detector and the drum at the distance d_0.

If the angular count rate distribution is homogeneous and if the gamma attenuation properties of the drum segment cannot be determined, then the activity of the corresponding isotope in the drum segment is calculated assuming an homogeneous matrix with the apparent density ρ_m as (Filß, 1995)

$$A = \frac{T_{\gamma}(\theta)_{mean}}{I_{\gamma} \cdot \varepsilon_0 \cdot F_0 \cdot 1 - e^{((-\mu/\rho_m)\rho_m \cdot (R-d_w))}} e^{((\mu/\rho_w)\rho_w \cdot d_w)} \tag{15}$$

The relative uncertainty for the activity calculated by Eq. (14) or (15) is estimated from the mean standard deviation of $T_{\gamma}(\theta)_{mean}$.

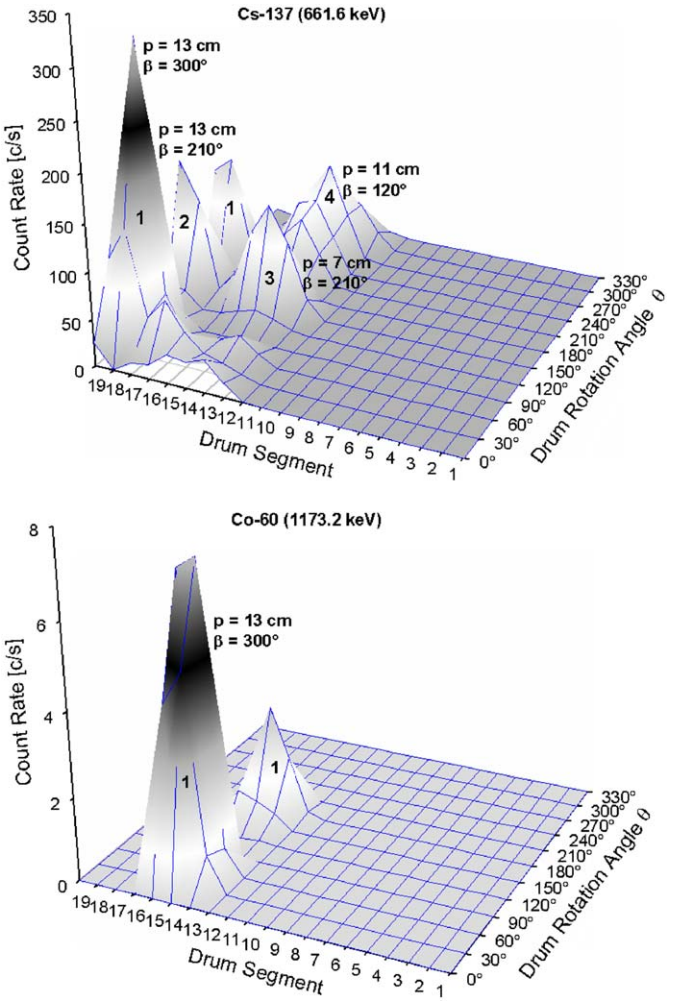

Fig. 2. Count rate distribution of Cs-137 (upper diagram) and Co-60 (lower diagram) measured for a drum with an apparent waste density of 2.63 g/cm^3. The determined radial and angular positions of the 'hot spots' are indicated on the diagrams. The counting time is 15 s per sector.

3. Application

The improved method was applied to the quantification of non-uniform distributed Cs-137 and Co-60 activities in 13 real waste drums (200 L). These drums were selected from a batch of drums with a typical signature of heterogeneous activity and matrix distribution. The waste matrix was made of lead canisters embedded in concrete containing dismounted radioactive sources for industrial application of well known activity. Based on *a priori* information, the mass of lead was ranging between 142 and 470 kg. The apparent density of the waste ρ_m determined by weighing was ranging between 2.61 and 4.04 g/cm^3. The drum height was 80 cm, the drum radius R was 28.15 cm and the wall thickness d_w was 0.15 cm. The waste drums were assayed by means of segmented gamma scanning with stepwise drum rotation. For that, the drums were subdivided into 20 equidistant segments and each segment rotation was subdivided into 12 sectors ($\Delta\theta = 30^{\circ}$) for which complete γ-spectra were measured and stored. The gamma-emitting isotopes were detected with a high resolution HPGe coaxial detector, 30% relative efficiency, shielded by means of a lead cylinder with a cylindrical collimation window. The length L_{col} and the radius R_{col} of the detector collimator were 20.5 and 2 cm, respectively. The thickness of the lead collimator was 9 cm. The distance of the drum segment centre from the centre of the detector surface d_0 was 74.65 cm. From this counting geometry, the volume of a drum segment seen by the collimated detector was 9769 cm^3 and the parameter F_0 was 166.63 cm^2. The detector was connected to a digital electronics DSPEC PLUS™ (ORTEC) for signal processing and the spectra were recorded with GAMMAVISION®-32 (ORTEC). The assay time was 1 h i.e. 15 s for each sector corresponding to the assay time set for routine scanning of drums. The gamma scanner was operated via a PC-based system with the software SCANNER 32 which was designed in collaboration with a professional software engineering company (HM Ingenieurbüro Marschelke) to support all aspects of the gamma scanning such as: full hardware control for detector lifting and drum rotation, nuclear instrumentation control for gamma-spectrometry and dose rate measurements, visualization of measurement progress (engine's status, spectral data, gamma count rate and dose rate distribution), data evaluation and analysis (spectrum analysis, activity determination) and result reporting and archiving. Detailed technical specifications of the gamma scanner employed for the routine characterization of radioactive waste drums may be found elsewhere (Report WG-A-01, 1998).

The angular dependent count rate distributions measured at 661.6 keV for Cs-137 and at 1173.2 keV for Co-60 were used to determine the activity of the isotopes. Numerical simulations

Table 1
Radiological parameters used to simulate the angular dependent count rate distributions.

Isotope	Cs-137	Co-60
E_γ (keV)	611.6	1173.2
I_γ (%)	85.1	99.97
ε_0 (%)	62.335×10^{-4}	40.900×10^{-4}
μ/ρ_m, μ/ρ_a (concrete) (cm^2/g)	77.551×10^{-3}	58.943×10^{-3}
μ/ρ_s, μ/ρ_c (lead) (cm^2/g)	111.22×10^{-3}	61.987×10^{-3}
μ/ρ_w (iron) (cm^2/g)	73.499×10^{-3}	55.263×10^{-3}

were performed with a computer program written in Visual Basic and running as a macro file under the software SigmaPlot® 8.0.2 (SYSTAT Sofware Inc.). The presence of 'hot spots' in drum segments was obtained from the statistical treatment of the measured angular dependent count rate distributions taking into account that a second maximum of the count rate at θ+180° could correspond to a maximum of the count rate observed at θ. Due to the low spatial resolution of the collimated detector it was assumed that no more than two 'hot spots' of the same isotope could coexist in a drum segment. The radial position of the sources p_i was varied from 1 cm to $(R-d_s-d_w)$ cm with a step of 2 cm. The angular position of the sources β_i was varied from 0° to 330° with a step of 30°. The mean thickness of the passive matrix d_s was varied from 0 to 20 cm with a step of 0.5 cm. The density of the active matrix ρ_a was restricted to vary between 1 g/cm^3 and the apparent waste density ρ_m. Matrix configurations leading to negatives values of ρ_a were systematically rejected. The radiological parameters used to simulate the count rate distributions of Cs-137 and Co-60 are given in Table 1. The densities of iron and lead are 7.63 and 11.34 g/cm^3, respectively. Additionally, the activity was calculated assuming a homogeneous density distribution using the apparent waste density ρ_m, setting thus the mean thickness of the passive matrix d_s to zero.

4. Results and discussion

As examples, the angular dependent count rate distributions of Cs-137 and Co-60 measured for two drums with apparent waste densities of 2.63 and 3.64 g/cm^3 are shown in Figs. 2 and 3, respectively. The drum with the lowest waste density contained 5 Cs-137 sources (0.7, 235, 821, 1237 and 5195 MBq) and 2 Co-60 sources (0.1 and 22 MBq). The drum with the highest waste density contained 6 Cs-137 sources (0.3, 0.3, 3.11, 3.11, 3.8 and 17289 MBq) and 2 Co-60 sources (0.05 and 12585 MBq). The source activities above are given at the time of the measurement. The radial and angular positions of the 'hot spots' within the drum segments as a result of the numerical simulations are given also in Figs. 3 and 4. In the first drum, 4 'hot spots' for Cs-137 and 1 'hot spot' for Co-60 were identified. Two Cs-137-'hot spots' are positioned at a drum height of about 76 cm with the same radial position (13 cm) but different angular positions (210° and 300°). The two other Cs-137-'hot spots' and the Co-60-'hot spot' are positioned at a drum height of about 60 cm with different radial and angular positions: (7 cm, 210°) and (11 cm, 120°) for Cs-137 and (13 cm, 300°) for Co-60. In the second drum, 4 'hot spots' for Cs-137 and 2 'hot spots' for Co-60 were identified at drum heights between 24 and 68 cm with the same radial position (13 cm) but different angular positions: (60°, 90°, 180°, 240°) for Cs-137 and (60°, 330°) for Co-60. It may be noted that the maximum of the count rate for a 'hot spot' occurred at a drum rotation angle $\theta = 360°-\beta$, which corresponds to the closest distance between the 'hot spot' and the detector during drum rotation. A second

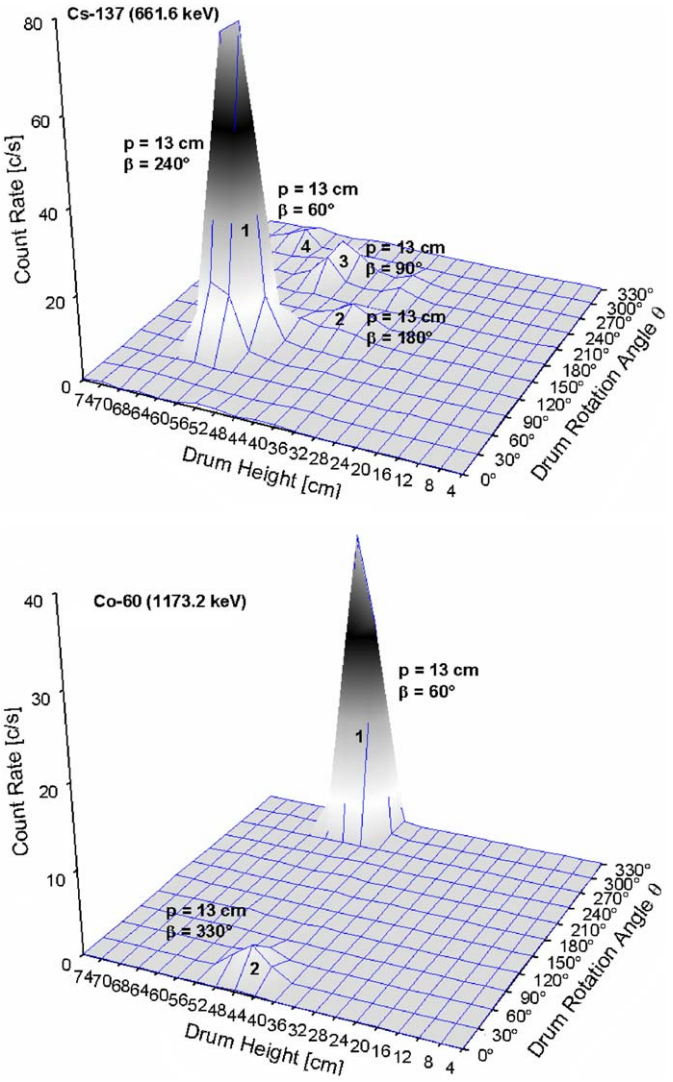

Fig. 3. Count rate distribution of Cs-137 (upper diagram) and Co-60 (lower diagram) measured for a drum with an apparent waste density of 3.64 g/cm^3. The determined radial and angular positions of the 'hot spots' are indicated on the diagrams. The counting time is 15 s per sector.

maximum may be observed at $\theta = 180°-\beta$ depending on the 'hot spot' activity and position, the γ-ray energy and the attenuation properties of the matrix. The radioactive sources with an activity lower than 1 MBq are not detected because of the lead shielding structures. The low intensity Co-60-'hot spot' in the second drum is probably a contamination as the source activity is only 50 kBq. The mean thickness of the lead shielding in the drum segments containing the 'hot spots' was found to be 4 cm for the first drum and to range between 3.5 and 6.5 cm for the second drum. The resulting activities of Cs-137 and Co-60 in the segments of the two drums are shown in Figs. 4 and 5. They reflect well the axial distribution of the isotopes within the drums.

The results obtained with the improved method compared to the true activity and to the activity calculated by the conventional method which assumes a homogeneous distribution of activity and matrix inside the drum segments are summarized for Cs-137 in Table 2 and for Co-60 in Table 3. The mean ratio of calculated to true activity is shown for the different methods applied in Fig. 6. The conventional method leads to a large underestimation of the activity since the non-uniform distribution of the isotopes and the shielding structures inside the drums are not considered. The

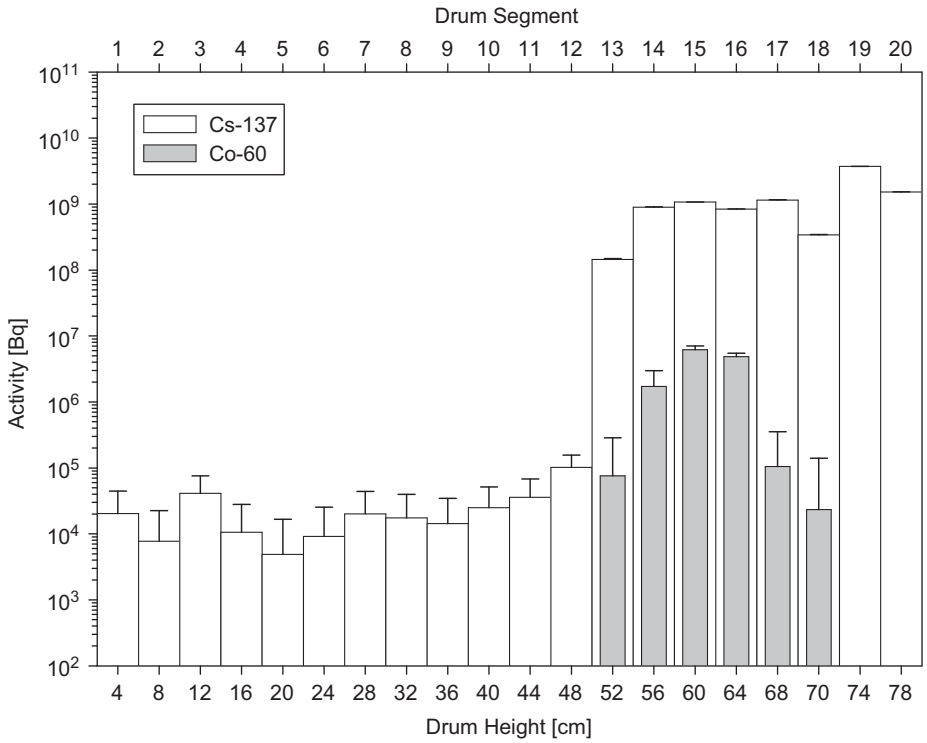

Fig. 4. Activity of Cs-137 and Co-60 in the segments of the drum with an apparent waste density of 2.63 g/cm^3. The activity is calculated for a non-uniform distribution of the isotopes and a heterogeneous sample matrix (see Fig. 2).

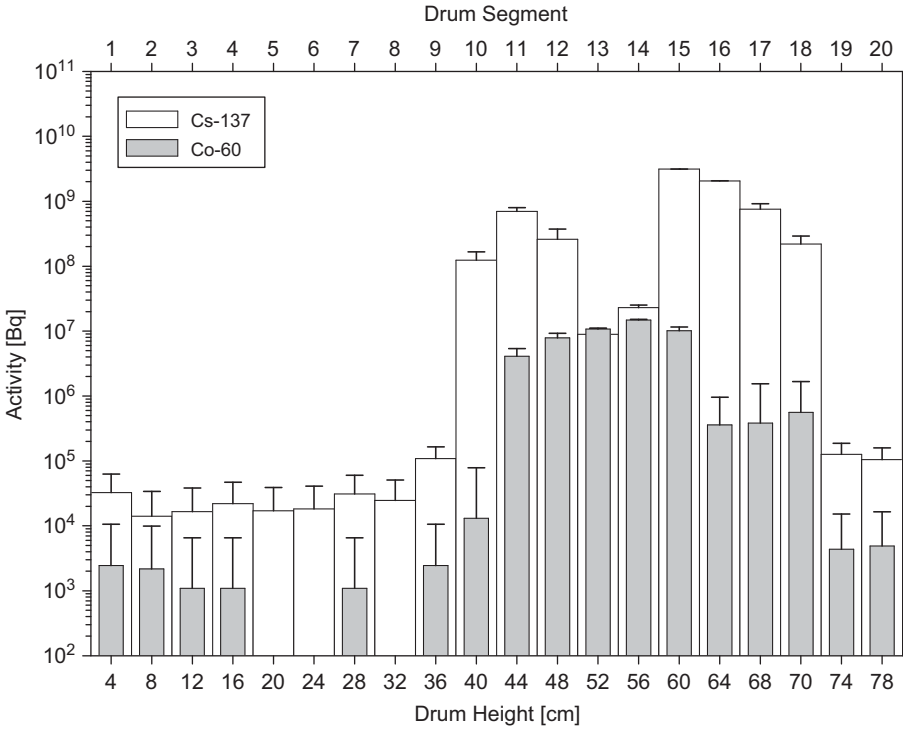

Fig. 5. Activity of Cs-137 and Co-60 in the segments of the drum with an apparent waste density of 3.64 g/cm^3. The activity is calculated for a non-uniform distribution of the isotopes and a heterogeneous sample matrix (see Fig. 3).

mean factor of underestimation is 586 for Cs-137 and 16 for Co-60. The activity of Cs-137 is much more underestimated compared to that of Co-60 due to a higher absorption of the γ-rays of Cs-137 by the lead shielding structures inside the waste. By applying the improved method for a *homogeneous* waste matrix, the activity values are somewhat higher as the non-uniform

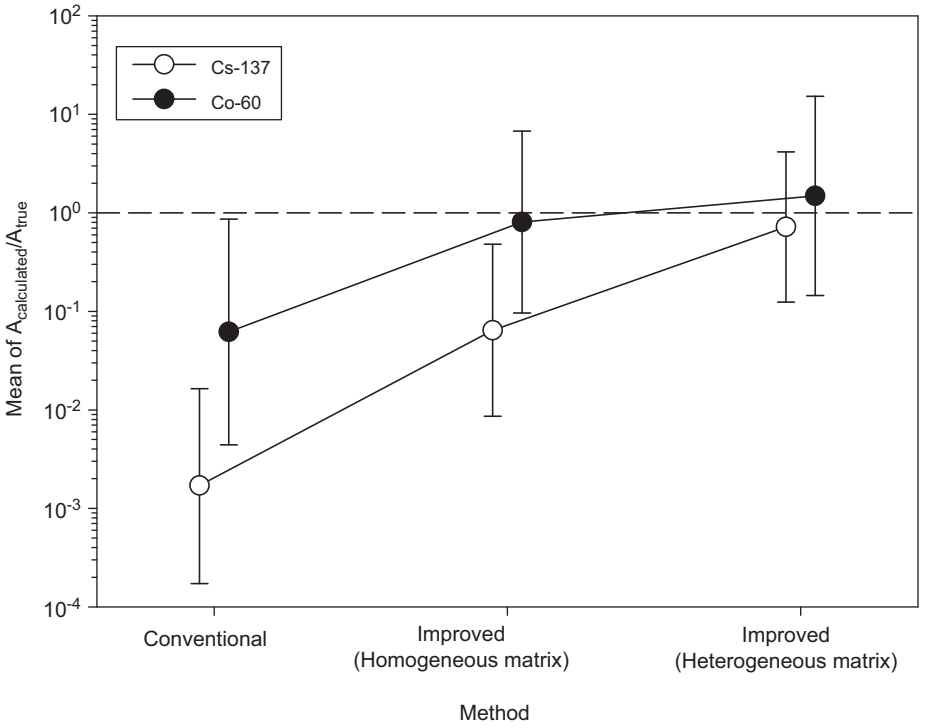

Fig. 6. Mean ratio of the calculated to true activity for the different methods applied.

Table 2
Results for the determination of the Cs-137 activity in the investigated radioactive waste drums by the conventional and improved method.

Cs-137 Activity in Bq					
Drum no.	Waste density (g/cm^3)	True activity	Conventional method	Improved method	
				Homogeneous matrix	Heterogeneous matrix
1	3.99	4.68×10^{10}	$1.48^{+0.59}_{-0.59} \times 10^{8}$	$2.65^{+0.58}_{-0.58} \times 10^{9}$	$4.27^{+0.94}_{-0.94} \times 10^{10}$
2	2.94	6.59×10^{10}	$1.42^{+0.22}_{-0.22} \times 10^{9}$	$1.81^{+1.61}_{-1.61} \times 10^{10}$	$6.08^{+5.41}_{-5.41} \times 10^{10}$
3	3.64	1.73×10^{10}	$8.08^{+2.98}_{-2.98} \times 10^{6}$	$2.27^{+2.51}_{-1.20} \times 10^{8}$	$7.30^{+8.10}_{-3.87} \times 10^{9}$
4	2.63	7.49×10^{9}	$6.70^{+0.94}_{-0.94} \times 10^{7}$	$7.97^{+12.67}_{-4.86} \times 10^{8}$	$9.68^{+15.39}_{-5.90} \times 10^{9}$
5	2.61	3.46×10^{11}	$1.69^{+0.29}_{-0.29} \times 10^{8}$	$2.19^{+2.10}_{-2.10} \times 10^{9}$	$1.10^{+1.06}_{-1.06} \times 10^{11}$
6	3.47	1.58×10^{11}	$4.40^{+0.46}_{-0.46} \times 10^{8}$	$3.49^{+5.06}_{-2.06} \times 10^{10}$	$4.54^{+6.58}_{-2.68} \times 10^{11}$
7	3.48	9.08×10^{10}	$1.16^{+0.12}_{-0.12} \times 10^{9}$	$7.49^{+13.56}_{-4.79} \times 10^{10}$	$9.60^{+17.38}_{-6.14} \times 10^{11}$
8	3.66	4.48×10^{11}	$4.87^{+0.81}_{-0.81} \times 10^{8}$	$2.05^{+1.58}_{-1.58} \times 10^{10}$	$1.67^{+1.28}_{-1.28} \times 10^{11}$
9	4.04	9.86×10^{10}	$3.03^{+0.10}_{-0.10} \times 10^{7}$	$7.34^{+1.54}_{-1.54} \times 10^{9}$	$6.57^{+1.38}_{-1.38} \times 10^{10}$
10	3.57	6.99×10^{10}	$1.29^{+0.04}_{-0.04} \times 10^{7}$	$1.84^{+0.66}_{-0.66} \times 10^{9}$	$1.50^{+0.54}_{-0.54} \times 10^{10}$
11	2.68	2.02×10^{10}	$4.12^{+0.35}_{-0.35} \times 10^{9}$	$7.71^{+1.54}_{-1.54} \times 10^{10}$	$3.95^{+0.79}_{-0.79} \times 10^{11}$
12	2.71	2.93×10^{12}	$4.77^{+1.12}_{-1.12} \times 10^{8}$	$7.48^{+3.74}_{-3.94} \times 10^{9}$	$1.04^{+0.52}_{-0.52} \times 10^{11}$
13	3.61	3.83×10^{11}	$3.88^{+0.53}_{-0.53} \times 10^{7}$	$5.54^{+5.37}_{-5.37} \times 10^{9}$	$3.24^{+3.14}_{-3.14} \times 10^{10}$
Total		4.68×10^{12}	$8.58^{-1.04}_{-1.054} \times 10^{9}$	$2.53^{+2.08}_{-1.27} \times 10^{11}$	$2.42^{+2.75}_{-1.36} \times 10^{12}$

The true activity is the sum of the sources activities. The activity is given at the time of the measurement.

distributions of the isotopes are now taken into account. The activity of Cs-137 and Co-60 is underestimated by a mean factor of 16 and 1.2, respectively. This corresponds to a mean improvement factor of 37 for Cs-137 and of 13 for Co-60 with respect to the conventional method due to correction for the non-uniform distribution of the isotopes. The results of the improved method for a *heterogeneous* waste matrix considering the presence of the lead shielding structures show a much better agreement with the true value, demonstrating its applicability and the validity of the geometric model used to simulate the angular dependent count rate distributions. In this case, the activity of Cs-137 is underestimated by a mean factor of 1.4 and the activity of Co-60 overestimated by a mean factor of 1.5. The mean improvement factor due to the correction of the γ-rays absorption by the heterogeneous matrix is 11 for Cs-137 and 2 for Co-60 compared to the case of a homogeneous waste matrix.

Table 3
Results for the determination of the Co-60 activity in the investigated radioactive waste drums by the conventional and improved method.

Co-60 Activity in Bq					
Drum no.	Waste density (g/cm^3)	Tue activity	Conventional method	Improved method	
				Homogeneous matrix	Heterogeneous matrix
1	3.99	6.53×10^9	$1.55^{+0.06}_{-0.06} \times 10^7$	$6.60^{+13.10}_{-4.36} \times 10^8$	$6.83^{+13.70}_{-4.55} \times 10^8$
2	2.94	6.40×10^7	$5.47^{+1.53}_{-1.53} \times 10^7$	$2.57^{+5.45}_{-1.75} \times 10^8$	$3.57^{+7.59}_{-2.43} \times 10^8$
3	3.64	8.04×10^8	$3.14^{+1.36}_{-1.36} \times 10^6$	$3.01^{+12.25}_{-2.41} \times 10^7$	$4.90^{+19.94}_{-3.92} \times 10^7$
4	2.63	2.15×10^7	$6.38^{+2.28}_{-2.28} \times 10^5$	$4.56^{+8.48}_{-2.96} \times 10^6$	$1.21^{+2.42}_{-0.85} \times 10^7$
5	2.61	–	–	–	–
6	3.47	–	–	–	–
7	3.48	5.00×10^5	$2.82^{+1.26}_{-1.26} \times 10^5$	$3.17^{+3.39}_{-1.65} \times 10^6$	$1.63^{+1.96}_{-0.95} \times 10^7$
8	3.66	–	–	–	–
9	4.04	3.70×10^{10}	$1.29^{+0.05}_{-0.05} \times 10^8$	$6.96^{+14.82}_{-4.59} \times 10^9$	$7.08^{+15.10}_{-4.82} \times 10^9$
10	3.57	2.36×10^9	$6.47^{+0.79}_{-0.79} \times 10^7$	$1.39^{+4.09}_{-1.04} \times 10^9$	$3.92^{+11.55}_{-2.95} \times 10^9$
11	2.68	2.52×10^7	$4.15^{+0.36}_{-0.36} \times 10^7$	$4.27^{+10.42}_{-3.03} \times 10^8$	$4.46^{+10.88}_{-3.17} \times 10^8$
12	2.71	9.29×10^7	$5.87^{+0.79}_{-0.79} \times 10^7$	$3.46^{+14.25}_{-2.80} \times 10^8$	$8.91^{+36.75}_{-7.22} \times 10^8$
13	3.61	–	–	–	–
Total		4.70×10^{10}	$3.68^{+0.42}_{-0.42} \times 10^8$	$1.01^{+3.16}_{-0.69} \times 10^{10}$	$1.34^{+3.37}_{-0.96} \times 10^{10}$

The true activity is the sum of the sources activities. The activity is given at the time of the measurement.

5. Conclusion

A method to improve the reliability and accuracy of activity results in segmented gamma scanning of radioactive waste drums exhibiting non-uniform isotope and density distributions has been developed and validated. In comparison to the conventional method, the quality of the activity results obtained by the improved method is largely enhanced. However, the application of the method needs a good counting statistics for the analysis of the angular dependent count rate distributions, which depends on the 'hot spot' activity, the γ-ray energy and the attenuation properties of the waste matrix. The presence of internal shielding structures inside the waste drum may be obtained from *a priori* information and controlled by weighing. An implementation of the improved method to the gamma scanner operation software SCANNER 32 will be performed to enhance the routine quality checking of radioactive waste packages.

References

Filß, P., 1995. Relation between the activity of a high-density waste drum and its gamma count rate measured with an unshielded Ge-detector. Appl. Radiat. Isot. 46, 805.

Report WG-A-01, 1998. Synopsis of gamma scanning systems; comparison of gamma determining systems and measuring procedures for radioactive waste packages. In: Bücherl, T., Kaniciel, E., Lierse, Ch. (Eds.). European Network of Testing Facilities for the Quality Checking of Radioactive Waste Packages (ENTRAP).

Report WG-A-03, 2002. Non-destructive analyses for the quality checking of radioactive waste packages. In: van Velzen, L.P.M. (Ed.), Proceedings of the Workshop Past, Present and Future of QA/QC on Radioactive waste, NRG Petten, The Netherlands, 19 and 20 June 2002. European Network of Testing Facilities for the Quality Checking of Radioactive Waste Packages (ENTRAP).

Quoc Dung, T., 1997. Calculation of the systematic error and correction factors in gamma waste assay system. Ann. Nucl. Energy 24, 33.

Quoc Dung, T., 1998. Some theoretical results of gamma techniques for measuring large samples. Nucl. Instrum. Methods Phys. Res. A 416, 505.